J|A|C|S COMMUNICATIONS

Published on Web 11/22/2010

Tripodal Tris-tacn and Tris-dpa Platforms for Assembling Phosphate-Templated Trimetallic Centers

Rui Cao, Peter Müller, and Stephen J. Lippard*

Department of Chemistry, Massachusetts Institute of Technology, Cambridge, Massachusetts 02139, United States

Received September 11, 2010; E-mail: lippard@mit.edu

Abstract: Multidentate tripodal ligands, $N(CH_2\text{-}m\text{-}C_6H_4\text{-}CH_2tacn)_3$ (**L1**) and $N(CH_2\text{-}o\text{-}C_6H_4\text{-}CH_2N(CH_2py)_2)_3$ (**L2**), have been devised for assembling high-nuclearity metal clusters. By using the same tripodal platform with different ligand appendages, either triazacyclononanes or dipicolylamines, and functionalizing either the ortho or the meta positions on the tris(xylyl) linker arms, discrete trimetal phosphate units of relevance to phosphate-metabolizing trimetallic centers in biology were prepared. Four such compounds, $[(Cu^{II}Cl)_3(HPO_4)$**L1**$](PF_6)$ (**1**), $[(Cu^{II}Cl)_3(HAsO_4)$**L1**$](PF_6)$ (**2**), $Na_2[Mn^{III}_6Mn^{II}_2(H_2O)_2(HPO_4)_6(PO_4)_4($**L1**$)_2]$ (**3**), and $[Co^{II}_3(H_2PO_4)Cl_2(MeCN)$**L2**$](PF_6)_3$ (**4**), all containing three metal centers bound to a central phosphate or arsenate unit bridging oxygen atoms, have been synthesized and structurally characterized. These results demonstrate the propensity of this novel tripodal ligand platform, in the presence of phosphate or arsenate, to assemble $\{M_3(EO_4)\}$ units and thus structurally mimic trimetallic active sites of proteins involved in phosphate metabolism. Reactivity studies reveal that the tricopper complex **1** is more efficient than monocopper analogues in catalyzing the hydrolysis of 4-nitrophenyl phosphate.

Metalloproteins containing three metal ions at their active sites perform a variety of important biological functions,[1] including the four-electron reduction of dioxygen to water by laccase and other multicopper oxidases,[2−5] the hydrolysis of phosphoric acid monoesters,[6,7] phospholipids,[8,9] nucleotides,[10,11] and inorganic pyrophosphate[12,13] by enzymes having a diverse array of divalent metal ions, and the mediation of electron transfer by 3(4)Fe-4S-containing proteins.[14,15] Phosphoric acid derivatives, including phosphates, also play a dominant role in biology,[16] including metabolic energy storage as adenosine triphosphate and energy generation by metal phosphate ($MHPO_4$) chelates.[17−19] Phosphate mono- and diesters are important structural components of lipids and macromolecules of the genome, and protein function is widely regulated by reversible phosphorylation of amino acid side chains.

Many enzymes required for phosphate metabolism contain a trimetallic active site.[1] Such trimetallic centers in P1 nuclease,[10,11] alkaline phosphatases,[6,20,21] phospholipase C,[8,9] and inorganic pyrophosphatases[12,13] are responsible for cleavage of phosphate P−O bonds; the trimetallic centers in PhoU proteins are involved in inorganic phosphate uptake and regulation.[22,23] In addition, some proteins, like T5 flap endonuclease, have only two divalent metal ions bound in the active site in the absence of phosphates but bind a third metal ion in the presence of substrates,[24] which implies a weak association constant for the third metal and a templating effect of phosphate substrates in the protein active site. The use of three metal ions to hydrolyze phosphates is believed to anchor and orient them in a position best suited for bond cleavage. As shown in Scheme 1 (left), the X-ray structure of a family II pyrophosphatase

Scheme 1

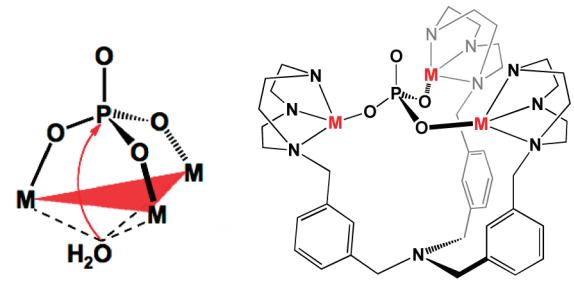

reveals an M_3 site bridged by the $\{PO_4\}$ unit, with each metal connected to one of the three O atoms of the phosphate and a nucleophilic water molecule below the M_3 plane.[13]

Many artificial phosphates/nucleases have been developed for applications in biotechnology and medicine, and multiple metal ions in a single molecule can endow unique activity.[25−30] Despite such achievements, however, no discrete structural model having a trimetallic center linked by a phosphate group within a single ligand framework to mimic the protein $\{M_3(PO_4)\}$ cores is available, to our knowledge.[7,13] We report here a tripodal platform in which ligand arms at either the meta or ortho positions of a tris(xylyl) scaffold can each bind one metal ion with phosphate or arsenate to self-assemble the desired core. The resulting structures have a tetrahedral anion binding to each metal through one of three facial oxygen atoms, similar to the coordination observed in protein active sites (Scheme 1, right). Four such complexes with different metal ions, ligand arms, and arm positions have been obtained, and all were structurally characterized, indicating the versatility of this tripodal platform. Moreover, reactivity studies reveal that the hydrolysis of 4-nitrophenyl phosphate is accelerated by the tricopper complex **1**, which is catalytically more efficient than its monocopper analogues.

In the course of developing multidentate ligands to coordinate trimetallic clusters, we found that a tribenzylamine scaffold provides the appropriate platform to draw three ligand arms together at the requisite spacing to accommodate a trimetal phosphate core. Crystallographic studies of a prototypical tripodal ligand backbone of this kind, $N(CH_2\text{-}p\text{-}C_6H_4\text{-}CONH_2)_3$ (Figure 1), the syntheses and properties of which are supplied in the Supporting Information, indicated that three symmetric ligand arms connected via para positions produce a flattened structure lacking the preorganized ligand environment suitable for assembling a trimetallic cluster. However, the structure revealed that ligand arms at the meta or ortho positions would produce the desired geometric configuration. We therefore placed three 1,4,7-triazacyclononane (tacn) ligand arms at the meta positions of the tribenzylamine platform, and this effort gave the novel tris-tacn tripodal cluster-forming ligand, $N(CH_2\text{-}m\text{-}C_6H_4\text{-}CH_2tacn)_3$ (**L1**) (syntheses and details in the Supporting Information). The choice of tacn ligand arms was based

10.1021/ja108212v

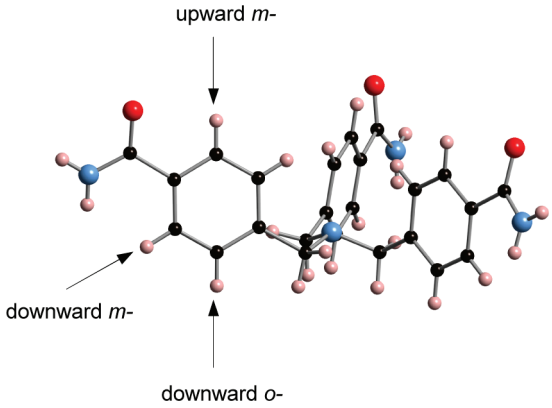

Figure 1. Ball-and-stick representation of the X-ray structure of a tripodal ligand model $N(CH_2\text{-}p\text{-}C_6H_4\text{-}CONH_2)_3$. The C, O, N, and H atoms are depicted in black, red, light blue, and light pink, respectively. The upward and downward meta positions and downward ortho position are labeled.

on the well-known facial coordination and high binding affinity of this unit for most transition metals.[31−33] Although ligands with two, three, or four tacn moieties linked by a phenyl group have been reported previously, in no case was a discrete trinuclear metal complex formed having a central phosphate bridge.[34−40]

Reaction of **L1** with $CuCl_2$ in the presence of HPO_4^{2-} under ambient conditions gave a clear blue solution after filtration. Addition of $NH_4(PF_6)$ to this clear solution and subsequent evaporation in air afforded crystalline prisms of $[(Cu^{II}Cl)_3(HPO_4)\mathbf{L1}](PF_6)$ (**1**). Complex **1** crystallizes in the trigonal space group $R\bar{3}$, with the monocationic cluster having a crystallographically required C_3 axis passing through the tetrahedral phosphate (O2 and P1) and nitrogen (N1) atoms (Figure 2). Each of the three symmetric ligand arms of **L1** coordinates one Cu(II) atom using three N atoms of the tacn moiety, and the three Cu atoms are bridged by the phosphate group with each Cu connected to one of the three facial oxygen atoms. A terminal chloride ligand on each Cu completes the coordination sphere and results in a distorted square-pyramidal geometry with the tertiary nitrogen atom (N2) at the apex (Cu1−N2, 2.256(3) Å). The fourth, uncoordinated oxygen atom (O2) of the phosphate is protonated, as revealed by the longer P1−O2 bond distance of 1.585(5) Å compared to P1−O1 = 1.516(2) Å. Monoprotonation of O2 is further confirmed by charge balance, with one PF_6^- counterion per trimetallic cluster being located both in the X-ray structure and by elemental analysis.

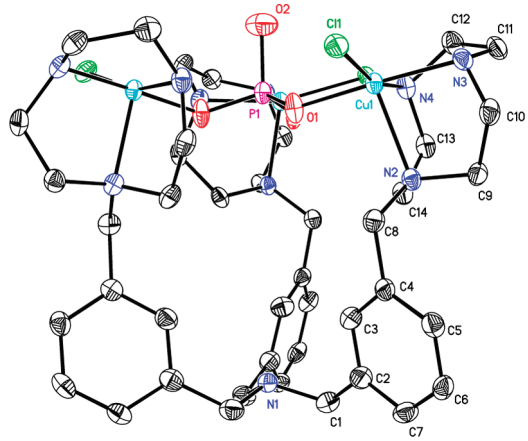

Figure 2. Thermal ellipsoid plot (50% probability) of the X-ray structure of complex **1**. The C_3 axis passes through O2, P1, and N1 atoms. Hydrogen atoms are omitted for clarity.

The molecular structure of **1** demonstrates that the tacn-based tripodal ligand $N(CH_2\text{-}m\text{-}C_6H_4\text{-}CH_2tacn)_3$ (**L1**) can bind three metal centers to afford the $\{(CuCl)_3(HPO_4)\}^+$ core in the presence of phosphate ion. Although, as shown in Figure 1, the ligand arms at the meta positions of the tribenzylamine linker can have either an upward or a downward orientation, the templating effect of the phosphate group selects the former to afford the desired trimetallic core. This conclusion is supported by studies of the ligand precursor $N(CH_2\text{-}m\text{-}C_6H_4\text{-}CH_2Br)_3$, in which the three bromomethyl arms adopt a downward orientation in the solid state (Figure S2, Supporting Information). Presumably, this geometric configuration is thermodynamically more stable prior to introduction of the phosphate anion to form **1**.

The arsenic analogue of **1** was also synthesized and structurally characterized. Replacement of HPO_4^{2-} with $HAsO_4^{2-}$ in the reaction of **L1** and $CuCl_2$, followed by addition of PF_6^- anion, gave small crystalline cubes of $[(Cu^{II}Cl)_3(HAsO_4)\mathbf{L1}](PF_6)$ (**2**). The structure matches that of the phosphate analogue (Figure S5, Supporting Information), in which a $\{(CuCl)_3(HAsO_4)\}^+$ core is coordinated by **L1** with each Cu(II) bound to three N atoms of a tacn-based ligand arm. The monocationic cluster has C_3 symmetry, and its charge is balanced by a PF_6^- counterion. The As−O distances (As1−O1 1.576(8) Å, As1−O2 1.623(17) Å) are longer than the P−O distances (P1−O1 = 1.516(2) Å, P1−O2 = 1.585(5) Å), a result consistent with the larger ionic radius of As(V) vs P(V).

Reaction of ligand **L1** with the dinuclear manganese complex $[Mn^{III}_2(\mu\text{-}O)(\mu\text{-}OAc)_2(bpy)_2Cl_2]$ in the presence of HPO_4^{2-} gave $Na_2[Mn^{III}_6Mn^{II}_2(H_2O)_2(HPO_4)_6(PO_4)_4(\mathbf{L1})_2]$ (**3**) as red crystalline prisms. Crystallographic studies revealed a remarkable octamanganese cluster flanked by two symmetry-equivalent **L1** ligands and overall C_i site symmetry (Figure 3). Alternatively, the structure of **3** can be described as a dimer of two symmetry-equivalent trimetallic $[Mn^{III}_3(HPO_4)_3(PO_4)_2\mathbf{L1}]^{3-}$ units, hereafter $\{Mn_3\mathbf{L1}\}^{3-}$, connected by two additional Mn atoms. In each $\{Mn_3\mathbf{L1}\}^{3-}$ unit, three manganese atoms are each coordinated by one tacn-based ligand arm through its three nitrogen atoms and additionally linked by a phosphate group (P1). The resulting $\{Mn_3(PO_4)\}^{6+}$ core is thus stabilized within the tripodal framework of ligand **L1**. The ligand arms in **3** are directed in the upward orientation, thereby resembling the geometric configuration observed in the structures of **1** and **2**.

In each $\{Mn_3\mathbf{L1}\}^{3-}$ unit, Mn1 has a terminal monodentate phosphate group (P2) and an aqua ligand to complete a six-coordinate, octahedral environment. The Mn2 and Mn3 atoms are each linked to the Mn4 atom through a bidentate bridging phosphate group (P4 and P3, respectively) and another such group (P5 and P5, respectively) that also uses one of its coordinated oxygen atoms to bridge to a third Mn atom. The Mn4 atom additionally binds to a fourth oxygen atom supplied by the P1 phosphate. The binding pattern of the resulting inorganic $\{Mn_8(HPO_4)_6(PO_4)_4\}^{2-}$ core is also depicted in Figure 3. A crystallographically imposed inversion center is located at the midpoint of the Mn4−Mn4 vector.

The three Mn atoms in the $\{Mn_3\mathbf{L1}\}^{3-}$ unit are all in the +3 oxidation state, as established by a bond valence sum (BVS) analysis as well as the existence of a Jahn−Teller elongation axis, typical of high-spin d^4 Mn(III) ions. The central Mn4 atoms, however, have a d^5 Mn(II) electronic configuration (BVS = 2.05), Mn(II) probably forming by disproportionation of Mn(III). Careful examination of the phosphate groups indicated the presence of six HPO_4^{2-} and four PO_4^{3-} units. Taken together, these considerations establish the formula as $[Mn^{III}_6Mn^{II}_2(H_2O)_2(HPO_4)_6(PO_4)_4(\mathbf{L1})_2]^{2-}$, with two Na^+ counterions.

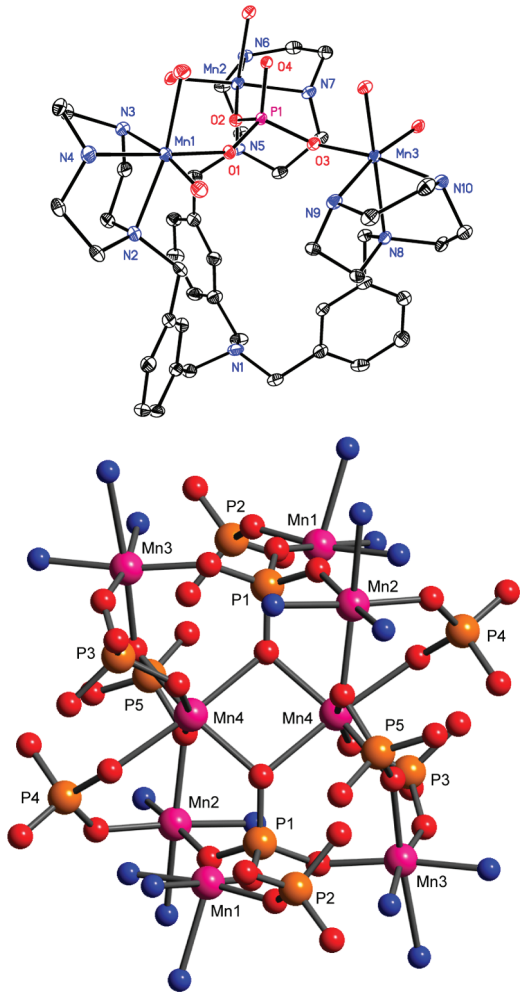

Figure 3. Thermal ellipsoid plot (30% probability) of the $\{Mn_3\mathbf{L1}\}^{3-}$, omitting some atoms of the P2, P3, P4, and P5 phosphate groups, subunit of complex **3** (top). Ball-and-stick representation of the $\{Mn_8(HPO_4)_6(PO_4)_4\}^{2-}$ core cluster of **3** (bottom). In the bottom part, the ligand backbone of **L1** is omitted. The Mn, P, O, and N atoms are shown in purple, orange, red, and blue, respectively.

A related trinucleating ligand based on the same tribenzylamine platform has been prepared. As noted from the structure of $N(CH_2\text{-}p\text{-}C_6H_4\text{-}CONH_2)_3$, ligand arms at the ortho positions can also give rise to a preorganized environment capable of forming a trimetallic center. We therefore prepared $N(CH_2\text{-}o\text{-}C_6H_4\text{-}CH_2N(CH_2py)_2)_3$ (**L2**), in which three dipicolylamine (dpa) ligand arms were appended to ortho positions in the tribenzylamine platform. The synthesis and details are available in the Supporting Information. Reaction of **L2** and $CoCl_2$ in the presence of $H_2PO_4^-$ gave a clear pink-purple solution. Addition of $NH_4(PF_6)$ to the reaction solution and vapor diffusion using diethyl ether at room temperature afforded crystalline purple prisms of $[Co^{II}_3(H_2PO_4)Cl_2(MeCN)\mathbf{L2}](PF_6)_3$ (**4**). In **4**, three Co(II) atoms, the oxidation states of which are supported by a BVS calculation (Supporting Information), are each bound by one **L2** dpa ligand appendage through three N atoms and linked by a central $H_2PO_4^-$ group (Figure 4). Co1 has a trigonal bipyramidal coordination sphere with a terminal Cl ligand at the apex trans to the tertiary nitrogen atom (N2). Co2 and Co3 are further bridged by a Cl^- ligand (Cl2). Co2 also has trigonal bipyramidal stereochemistry, with Cl2 at the apex trans to the tertiary nitrogen atom (N5), whereas Co3 is six-coordinate, with a terminal MeCN ligand trans to the tertiary nitrogen atom (N8). The resulting trimetallic cluster $[Co^{II}_3(H_2PO_4)Cl_2(MeCN)\mathbf{L2}]^{3+}$ is charge-balanced by three PF_6^- ions that were also located in the X-ray structure.

The structures of **1**−**4** represent the first examples in which a trimetal phosphate/arsenate unit is stabilized in a discrete ligand environment. As such, they serve as structural mimics of trimetal phosphate enzyme active sites.[7,13] The occurrence of this unit in diverse complexes illustrates the value of using the new trinucleating ligands in conjunction with bridging tetrahedral anions like phosphate or arsenate.

In order to examine the potential for such complexes to serve as metallohydrolase catalysts, we studied the hydrolysis of 4-nitrophenyl phosphate in the presence of the tricopper(II) complex **1**. As deduced by a high-resolution ESI-MS measurement (Figure S9, Supporting Information), the monocationic cluster **1** stays intact upon dissolution. This hydrolytic reaction produces inorganic phosphate and 4-nitrophenol, which can be readily detected spectroscopically by its strong electronic absorption at ∼400 nm).[41,42] Kinetic studies revealed that the hydrolysis of 4-nitrophenyl phosphate is accelerated by **1** (Figure S10, Supporting Information). We also investigated this hydrolysis reaction using the mononuclear copper tacn complex $[Cu(tacn)Cl_2]$, which structurally resembles a single ligand arm of **1**. The observed hydrolysis rate for **1** is 12 times greater than that of $[Cu(tacn)Cl_2]$ at equimolar copper concentrations, which suggests that the three copper atoms in close proximity may work together with greater efficiency than mononuclear copper species in catalyzing the hydrolysis of 4-nitrophenyl phosphate.

In conclusion, by using tripodal ligand $N(CH_2\text{-}m\text{-}C_6H_4\text{-}CH_2tacn)_3$ (**L1**) or $N(CH_2\text{-}o\text{-}C_6H_4\text{-}CH_2N(CH_2py)_2)_3$ (**L2**), trimetal phosphate or arsenate units that mimic natural sites in phosphate-metabolizing enzymes were accessed in discrete molecular systems. Four compounds, all containing such a trimetallic core, were prepared and structurally characterized: $[(Cu^{II}Cl)_3(HPO_4)\mathbf{L1}](PF_6)$ (**1**), $[(Cu^{II}Cl)_3(HAsO_4)\mathbf{L1}](PF_6)$ (**2**), $Na_2[Mn^{III}_6Mn^{II}_2(H_2O)_2(HPO_4)_6(PO_4)_4(\mathbf{L1})_2]$ (**3**), and $[Co^{II}_3(H_2PO_4)Cl_2(MeCN)\mathbf{L2}](PF_6)_3$ (**4**). In all four compounds, three metal ions are each bound by one arm of the tripodal ligand through three N atoms and further linked by a tetrahedral phosphate, protonated phosphate, or protonated arsenate group. The resulting structures reprise features of the phosphate-bridged trimetallic active sites in several proteins involved in phosphate metabolism.[7,13] Complex **1** catalyzes the hydrolysis of 4-nitrophenyl phosphate with a greater efficiency than its mononuclear Cu(II) tacn analogue, a result sug-

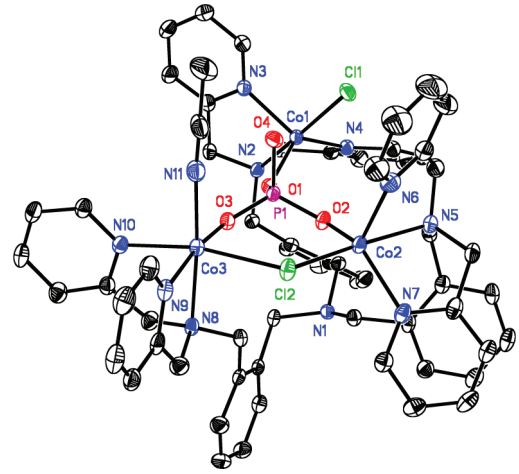

Figure 4. Thermal ellipsoid plot (50% probability) of the X-ray structure of **4**.

gesting that three copper atoms in close proximity provide an advantage for effecting this chemistry.

Acknowledgment. This work was supported by a grant from the Camille and Henry Dreyfus Foundation. We thank Dr. William H. Armstrong for helpful discussions. This paper is dedicated to Prof. Dr. Karl Wieghardt on the occasion of his retirement.

Supporting Information Available: Complete synthesis and characterization of the tripodal model complex $N(CH_2\text{-}p\text{-}C_6H_4\text{-}CONH_2)_3$, tripodal ligands **L1** and **L2**, and metal complexes **1**−**4**; hydrolysis studies of 4-nitrophenyl phosphate; Schemes S1−S3, Tables S1−S8, and Figures S1−S10; X-ray data as CIF files for $N(CH_2\text{-}p\text{-}C_6H_4\text{-}CONH_2)_3$, $N(CH_2\text{-}m\text{-}C_6H_4\text{-}CH_2Br)_3$, $N(CH_2\text{-}o\text{-}C_6H_4\text{-}CH_2OH)_3$, $[Mn^{III}_2(\mu\text{-}O)(\mu\text{-}OAc)_2(bpy)_2Cl_2]$, and metal complexes **1**−**4**. This material is available free of charge via the Internet at http://pubs.acs.org.

References

(1) Fenton, D. E.; Okawa, H. *J. Chem. Soc., Dalton Trans.* **1993**, 1349–1357.
(2) Sundaram, U. M.; Zhang, H. H.; Hedman, B.; Hodgson, K. O.; Solomon, E. I. *J. Am. Chem. Soc.* **1997**, *119*, 12525–12540.
(3) Yoon, J.; Liboiron, B. D.; Sarangi, R.; Hodgson, K. O.; Hedman, B.; Solomon, E. I. *Proc. Natl. Acad. Sci. U.S.A.* **2007**, *104*, 13609–13614.
(4) Quintanar, L.; Stoj, C.; Taylor, A. B.; Hart, P. J.; Kosman, D. J.; Solomon, E. I. *Acc. Chem. Res.* **2007**, *40*, 445–452.
(5) Augustine, A. J.; Kjaergaard, C.; Qayyum, M.; Ziegler, L.; Kosman, D. J.; Hodgson, K. O.; Hedman, B.; Solomon, E. I. *J. Am. Chem. Soc.* **2010**, *132*, 6057–6067.
(6) Stec, B.; Holtz, K. M.; Kantrowitz, E. R. *J. Mol. Biol.* **2000**, *299*, 1303–1311.
(7) Omi, R.; Goto, M.; Miyahara, I.; Manzoku, M.; Ebihara, A.; Hirotsu, K. *Biochemistry* **2007**, *46*, 12618–12627.
(8) Hough, E.; Hansen, L. K.; Birknes, B.; Jynge, K.; Hansen, S.; Hordvik, A.; Little, C.; Dodson, E.; Derewenda, Z. *Nature* **1989**, *338*, 357–360.
(9) Hansen, S.; Kristian, L.; Hough, H.; Hough, E. *J. Mol. Biol.* **1992**, *225*, 543–549.
(10) Lahm, A.; Volbeda, A.; Suck, D. *J. Mol. Biol.* **1990**, *215*, 207–210.
(11) Volbeda, A.; Lahm, A.; Sakiyama, F.; Suck, D. *EMBO J.* **1991**, *10*, 1607–1618.
(12) Cooperman, B. S.; Baykov, A. A.; Lahti, R. *Trends Biochem. Sci.* **1992**, *17*, 262–266.
(13) Fabrichniy, I. P.; Lehtiö, L.; Tammenkoski, M.; Zyryanov, A. B.; Oksanen, E.; Baykov, A. A.; Lahti, R.; Goldman, A. *J. Biol. Chem.* **2007**, *282*, 1422–1431.
(14) Beinert, H.; Thomson, A. J. *Arch. Biochem. Biophys.* **1983**, *222*, 333–361.
(15) Holm, R. H. *Adv. Inorg. Chem.* **1992**, *38*, 1–71.
(16) Bowler, M. W.; Cliff, M. J.; Waltho, J. P.; Blackburn, G. M. *New J. Chem.* **2010**, *34*, 784–794.
(17) van Veen, H. W.; Abee, T.; Kortstee, G. J. J.; Konings, W. N.; Zehnder, A. J. B. *Biochemistry* **1994**, *33*, 1766–1770.
(18) van Veen, H. W.; Abee, T.; Kortstee, G. J. J.; Konings, W. N.; Zehnder, A. J. B. *J. Biol. Chem.* **1994**, *269*, 16212–16216.
(19) Konings, W. N.; Lolkema, J. S.; Poolman, B. *Arch. Microbiol.* **1995**, *164*, 235–242.
(20) Kim, E. E.; Wyckoff, H. W. *J. Mol. Biol.* **1991**, *218*, 449–464.
(21) Le Du, M. H.; Stigbrand, T.; Taussig, M. J.; Ménez, A.; Stura, E. A. *J. Biol. Chem.* **2001**, *276*, 9158–9165.
(22) Steed, P. M.; Wanner, B. L. *J. Bacteriol.* **1993**, *175*, 6797–6809.
(23) Liu, J. Y.; Lou, Y.; Yokota, H.; Adams, P. D.; Kim, R.; Kim, S. H. *J. Biol. Chem.* **2005**, *280*, 15960–15966.
(24) Syson, K.; Tomlinson, C.; Chapados, B. R.; Sayers, J. R.; Tainer, J. A.; Williams, N. H.; Grasby, J. A. *J. Biol. Chem.* **2008**, *283*, 28741–28746.
(25) Komiyama, M.; Kina, S.; Matsumura, K.; Sumaoka, J.; Tobey, S.; Lynch, V. M.; Anslyn, E. V. *J. Am. Chem. Soc.* **2002**, *124*, 13731–13736.
(26) Humphreys, K. J.; Karlin, K. D.; Rokita, S. E. *J. Am. Chem. Soc.* **2002**, *124*, 8055–8066.
(27) Cacciapaglia, R.; Casnati, A.; Mandolini, L.; Peracchi, A.; Reinhoudt, D. N.; Salvio, R.; Sartori, A.; Ungaro, R. *J. Am. Chem. Soc.* **2007**, *129*, 12512–12520.
(28) Williams, N. H.; Takasaki, B.; Wall, M.; Chin, J. *Acc. Chem. Res.* **1999**, *32*, 485–493.
(29) Molenveld, P.; Engbersen, J. F. J.; Reinhoudt, D. N. *Chem. Soc. Rev.* **2000**, *29*, 75–86.
(30) Morrow, J. R.; Iranzo, O. *Curr. Opin. Chem. Biol.* **2004**, *8*, 192–200.
(31) Hartman, J. A. R.; Rardin, R. L.; Chaudhuri, P.; Pohl, K.; Wieghardt, K.; Nuber, B.; Weiss, J.; Papaefthymiou, G. C.; Frankel, R. B.; Lippard, S. J. *J. Am. Chem. Soc.* **1987**, *109*, 7387–7396.
(32) Wieghardt, K.; Bossek, U.; Nuber, B.; Weiss, J.; Bonvoisin, J.; Corbella, M.; Vitols, S. E.; Girerd, J. J. *J. Am. Chem. Soc.* **1988**, *110*, 7398–7411.
(33) Bossek, U.; Weyhermüller, T.; Wieghardt, K.; Nuber, B.; Weiss, J. *J. Am. Chem. Soc.* **1990**, *112*, 6387–6388.
(34) Graham, B.; Fallon, G. D.; Hearn, M. T. W.; Hockless, D. C. R.; Lazarev, G.; Spiccia, L. *Inorg. Chem.* **1997**, *36*, 6366–6373.
(35) Farrugia, L. J.; Lovatt, P. A.; Peacock, R. D. *J. Chem. Soc., Dalton Trans.* **1997**, 911–912.
(36) Belousoff, M. J.; Graham, B.; Spiccia, L. *Eur. J. Inorg. Chem.* **2008**, 4133–4139.
(37) Spiccia, L.; Graham, B.; Hearn, M. T. W.; Lazarev, G.; Moubaraki, B.; Murray, K. S.; Tiekink, E. R. T. *J. Chem. Soc., Dalton Trans.* **1997**, 4089–4097.
(38) Graham, B.; Spiccia, L.; Fallon, G. D.; Hearn, M. T. W.; Mabbs, F. E.; Moubaraki, B.; Murray, K. S. *J. Chem. Soc., Dalton Trans.* **2002**, 1226–1232.
(39) Graham, B.; Hearn, M. T. W.; Junk, P. C.; Kepert, C. M.; Mabbs, F. E.; Moubaraki, B.; Murray, K. S.; Spiccia, L. *Inorg. Chem.* **2001**, *40*, 1536–1543.
(40) Battle, A. R.; Graham, B.; Spiccia, L.; Moubaraki, B.; Murray, K. S.; Skelton, B. W.; White, A. H. *Inorg. Chim. Acta* **2006**, *359*, 289–297.
(41) Tang, S. P.; Zhou, Y. H.; Chen, H. Y.; Zhao, C. Y.; Mao, Z. W.; Ji, L. N. *Chem. Asian J.* **2009**, *4*, 1354–1360.
(42) Steens, N.; Ramadan, A. M.; Absillis, G.; Parac-Vogt, T. N. *Dalton Trans.* **2010**, *39*, 585–592.

JA108212V